

Available online at www.sciencedirect.com**SciVerse ScienceDirect**

Advances in Space Research 48 (2011) 1942–1957

**ADVANCES IN
SPACE
RESEARCH**
(a COSPAR publication)
www.elsevier.com/locate/asr

The Radio Observatory on the Lunar Surface for Solar studies

T. Joseph W. Lazio^{a,b,*}, R.J. MacDowall^{c,b}, Jack O. Burns^{d,b}, D.L. Jones^{e,b}, K.W. Weiler^{a,b},
L. Demaio^c, A. Cohen^f, N. Paravastu Dalal^g, E. Polisensky^a, K. Stewart^a, S. Bale^h,
N. Gopalswamy^c, M. Kaiser^c, J. Kasperⁱ

^a Remote Sensing Division, Naval Research Laboratory, 4555 Overlook Ave. SW, Washington, DC 20375-5351, USA

^b NASA Lunar Science Institute, NASA Ames Research Center, Moffett Field, CA 94089, USA

^c NASA/Goddard Space Flight Center, Code 695, 8800 Greenbelt Rd., Greenbelt, MD 20771, USA

^d Center for Astrophysics and Space Astronomy, Dept. of Astrophysical & Planetary Science, University of Colorado, Boulder, CO 80309, USA

^e MIS 138-308, Jet Propulsion Laboratory, 4800 Oak Grove Dr., Pasadena, CA 91109, USA

^f The Johns Hopkins University, Applied Physics Laboratory, 11100 Johns Hopkins Rd., Laurel, MD 20723, USA

^g ASEE Engineering Fellow, 255 West 5th St, San Pedro, CA 90731, USA

^h Physics Dept. and Space Sciences Laboratory, University of California, Berkeley, CA 94720-7300, USA

ⁱ Harvard-Smithsonian Center for Astrophysics, Perkins 138, MS 58, 60 Garden Street, Cambridge, MA 02138, USA

Received 17 November 2010; received in revised form 12 July 2011; accepted 12 July 2011

Available online 24 July 2011

Abstract

The Radio Observatory on the Lunar Surface for Solar studies (ROLSS) is a concept for a near-side low radio frequency imaging interferometric array designed to study particle acceleration at the Sun and in the inner heliosphere. The prime science mission is to image the radio emission generated by Type II and III solar radio burst processes with the aim of determining the sites at and mechanisms by which the radiating particles are accelerated. Specific questions to be addressed include the following: (1) Isolating the sites of electron acceleration responsible for Type II and III solar radio bursts during coronal mass ejections (CMEs); and (2) Determining if and the mechanism(s) by which multiple, successive CMEs produce unusually efficient particle acceleration and intense radio emission. Secondary science goals include constraining the density of the lunar ionosphere by searching for a low radio frequency cutoff to solar radio emission and constraining the low energy electron population in astrophysical sources. Key design requirements on ROLSS include the operational frequency and angular resolution. The electron densities in the solar corona and inner heliosphere are such that the relevant emission occurs at frequencies below 10 MHz. Second, resolving the potential sites of particle acceleration requires an instrument with an angular resolution of at least 2°, equivalent to a linear array size of approximately 1000 m. Operations would consist of data acquisition during the lunar day, with regular data downlinks. No operations would occur during lunar night.

ROLSS is envisioned as an interferometric array, because a single aperture would be impractically large. The major components of the ROLSS array are 3 antenna arms arranged in a Y shape, with a central electronics package (CEP) located at the center. The Y configuration for the antenna arms both allows for the formation of reasonably high dynamic range images on short time scales as well as relatively easy deployment. Each antenna arm is a linear strip of polyimide film (e.g., Kapton™) on which 16 science antennas are located by depositing a conductor (e.g., silver). The antenna arms can be rolled for transport, with deployment consisting of unrolling the rolls. Each science antenna is a single polarization dipole. The arms also contain transmission lines for carrying the radio signals from the science antennas to the CEP. The CEP itself houses the receivers for the science antennas, the command and data handling hardware, and, mounted externally, the downlink antenna.

We have conducted two experiments relevant to the ROLSS concept. First, we deployed a proof-of-concept science antenna. Comparison of the impedance of the antenna feed points with simulations showed a high level of agreement, lending credence to the antenna concept. Second, we exposed a sample of space-qualified polyimide film, with a silver coating on one side, to temperature cycling and UV

* Corresponding author. Current address: M/S 138-308, Jet Propulsion Laboratory, California Institute of Technology, 4800 Oak Grove Dr., Pasadena, CA 91109, USA.

E-mail address: Joseph.Lazio@jpl.nasa.gov (T.J.W. Lazio).

exposure designed to replicate a year on the lunar surface. No degradation of the polyimide film's material or electric properties was found. Both of these tests support the notion of using polyimide-film based antennas.

The prime science mission favors an equatorial site, and a site on the limb could simplify certain aspects of the instrument design. A site on the lunar near side is sufficient for meeting the science goals. While the site should be of relatively low relief topography, the entire site does not have to be flat as the fraction of the area occupied by the antenna arms is relatively small ($\sim 0.3\%$). Further, the antenna arms do not have to lay flat as deviations of ± 1 m are still small relative to the observational wavelengths. Deployment could be accomplished either with astronauts, completely robotically, or via a combination of crewed and robotic means.

Future work for the ROLSS concept includes more exhaustive testing of the radio frequency (RF) and environmental suitability of polyimide film-based science antennas, ultra-low power electronics in order to minimize the amount of power storage needed, batteries with a larger temperature range for both survival and operation, and rovers (robotic, crewed, or both) for deployment.

The ROLSS array could also serve as the precursor to a larger array on the far side of the Moon for astrophysical and cosmological studies.

© 2011 COSPAR. Published by Elsevier Ltd. All rights reserved.

Keywords: Heliophysics; Instrumentation: interferometers; Moon; Particle acceleration; Radio astronomy

1. Introduction

Our view of the Universe at wavelengths longer than about 30 m (frequencies < 10 MHz) is impeded significantly by the Earth's ionosphere. These wavelengths correspond to frequencies comparable to or below plasma frequency of the ionosphere, so that any celestial radiation is reflected. The actual plasma frequency varies as a function of solar illumination, solar cycle, and even geomagnetic latitude, and there have been a series of attempts to exploit favorable conditions to observe from the ground at these wavelengths. In general, however, ground-based observations are not possible.

The lack of ionospheric transparency has motivated two astrophysical missions, Radio Astronomy Explorers 1 and 2 (RAE-1 and RAE-2); several solar missions, the most recent of which includes the STEREO mission; and radio receivers on a variety of planetary missions. Both RAE-1 and RAE-2, as well as essentially all of the solar missions, carried one to three monopole or dipole antennas, resulting in limited angular resolution. Considerable information about solar radio emissions have been extracted from dynamic spectra (intensity as a function of both time and frequency), and these few dipole instruments have also been useful for an initial assessment of the long-wavelength Universe. However, substantive questions remain, questions that will likely require substantially higher angular resolution than can be provided by a single dipole. Stimulated by the successes of RAE-1 and RAE-2, there have also been proposals for constellations of free-flying spacecraft, each with a single or crossed dipole antenna (Weiler, 1986; Weiler et al., 1988; Jones et al., 2000; MacDowall et al., 2005, 2006) that would provide higher angular resolution.

NASA has considered a variety of options for both a human and robotic return to the Moon. One option included sortie missions. The Apollo missions serve as the model for sortie missions, in that a small crew (2–4 people) land on the surface for a short period of time (~ 7 days) and then return to Earth. During their time on the surface, their

activities can include the deployment of experimental packages. A number of such packages were deployed during the Apollo missions, including retro-reflectors that continue to be used today to monitor the Earth–Moon distance and test theories of gravity (Dickey et al., 1994). However, the improvement in robotics capabilities, including autonomous operations, allows for the consideration of more complicated, completely robotic deployment of instrument packages.

As part of the Lunar Sortie Science Opportunities (LSSO) program, we carried out a concept study for the Radio Observatory for Lunar Sortie Science—since renamed to the Radio Observatory on the Lunar Surface for Solar studies (ROLSS)—a long-wavelength imaging radio interferometer having a primary science mission of resolving the locations of particle acceleration in solar radio bursts (Fig. 1). While similar in concept to a constellation of free-flying spacecraft, an array on the Moon has at least three advantages over a constellation. First, with the lunar surface as a structural support, the antenna locations can be determined permanently and they do not diverge with time. Second, mission operations and resource costs are not required to maintain the array configuration. Finally, the Moon blocks half the sky, simplifying the imaging.

This paper presents the results of our concept study of ROLSS and some initial proof-of-concept tests that we have conducted on the ROLSS concept. The plan of this paper is as follows. In Section 2 we present the science case for ROLSS; in Section 3 we describe the current baseline design, the experimental tests that we conducted, and the operations; in Section 4 we discuss siting and deployment; in Section 5 we present an initial technology roadmap toward realizing ROLSS, and in Section 6 we present our conclusions. Because this concept study was funded under a program designed to conduct science during human sorties, the concept was developed with the assumption of astronaut deployment, but an extension to a completely robotic deployment is obvious, and options are illustrated in Section 4. While the focus of this paper is on ROLSS

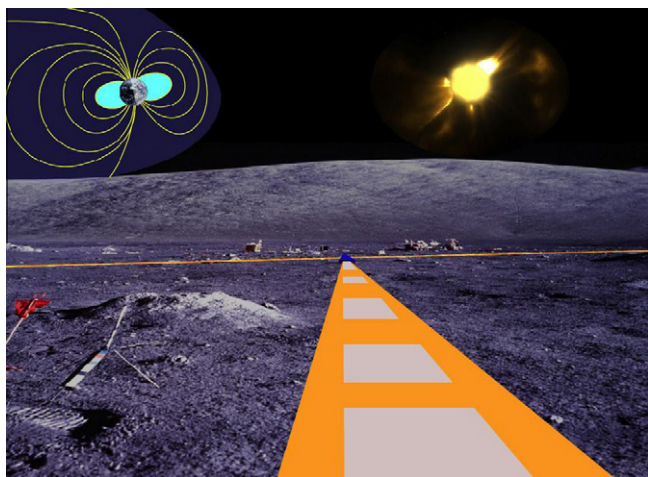


Fig. 1. Artist's illustration of the Radio Observatory on the Lunar Surface for Solar studies (ROLSS) deployed on the surface of the Moon. In the foreground is one of the three antenna arms, composed of a strip of polyimide film with single polarization dipole antennas deposited on it. In the distance are the other two arms as well as the central electronics package at the center of the arms. In this scenario, ROLSS is deployed as part of a crewed sortie, and other equipment associated with the sortie is visible near the center of the array. In a completely robotic deployment, it is likely that significantly fewer items would be present.

and the study of the inner heliosphere, the ROLSS array could also serve as the precursor for a future, larger radio telescope on the far side of Moon for astrophysical and cosmological studies (Carilli et al., 2007; Lazio et al., 2007, 2009).

2. Science

2.1. Particle acceleration

High-energy particle acceleration occurs in diverse astrophysical environments including the Sun and other stars, supernovae, black holes, and quasars. A fundamental problem is in understanding the mechanisms and sites of this acceleration, in particular the roles of shock waves and magnetic reconnection. Within the inner heliosphere—an interval of 1–10 solar radii (R_{\odot}) from the Sun—solar flares and coronal mass ejections (CMEs) are efficient particle accelerators.

Low frequency observations are an excellent remote diagnostic because electrons accelerated by these structures can produce intense radio bursts. The intensities of these bursts make them easy to detect, as well as providing information about the acceleration regions. The radio burst mechanisms discussed here involve emission at the local plasma frequency, $f_p \approx 9\sqrt{n_e}$ kHz, or its harmonics, where n_e is the electron density in cm^{-3} . With a model for n_e , f_p can be converted into a height above the corona, and changing f_p can be converted into radial speed.

Solar radio bursts are one of the primary remote signatures of electron acceleration in the inner heliosphere, and our focus is on two specific kinds, referred to as Type II and III radio bursts. Type II bursts originate from

supra-thermal electrons ($E > 100$ eV) produced at shocks. These shocks generally are produced by CMEs as they expand into the heliosphere with Mach numbers greater than unity. Emission from a Type II burst drops slowly in frequency as the shock moves away from the Sun into lower density regions at speeds of 400–2000 km s^{-1} . Type III bursts are generated by fast (2–20 keV) electrons from magnetic reconnection. As the fast electrons escape at a significant fraction of the speed of light into the heliosphere along magnetic field lines, they produce emission that drops in frequency rapidly.

Electron densities in the inner heliosphere mean that the relevant radiation emission frequencies are below 10 MHz (Leblanc et al., 1998; Mann et al., 1999), and Bougeret et al. (1995) present several examples that illustrate the active low-frequency radio environment in space, as observed by the *non-imaging* WAVES instrument on the Wind spacecraft.¹ Observations must be conducted from space because the ionosphere is opaque in this frequency range.

ROLSS will address three key scientific questions related to particle acceleration:

Acceleration at shocks: Observations of CMEs near Earth suggest electron acceleration generally occurs where the shock normal is perpendicular to the magnetic field (Bale et al., 1999), similar to acceleration at planetary bow shocks and other astrophysical sites. This geometry may be unusual in the corona, where the magnetic field is largely radial, as shown schematically in Fig. 2(a). However, geometric arguments suggest that the shocks at the front of CMEs generally have a quasi-parallel geometry (Q-||). Acceleration along the flanks of the CME, where the magnetic field-shock normal is quasi-perpendicular (Q- \perp) would seem to be a more likely location for the electron acceleration and Type II emission, but both Q-|| and Q- \perp have been proposed as mechanisms for Type II emission (e.g., Holman and Pesses, 1983; Mann and Luehr, 1994).

Electron and ion acceleration: Observations at 2–15 MHz made with the Wind spacecraft showed that complex Type III bursts (sometimes called Type III-L) are highly correlated with CMEs and intense (proton) solar energetic particle (SEP) events observed at 1 AU (Cane et al., 2002; Lara et al., 2003; MacDowall et al., 2003). While the association between Type III-L bursts, proton SEP events, and CMEs is now secure, the electron acceleration mechanism remains poorly understood. Two competing sites for the acceleration have been suggested: at shocks in front of a CME or in reconnection regions behind a CME (Fig. 2b).

CME interactions and solar energetic particle (SEP) intensity: Unusually intense radio emission can occur

¹ For more recent work, see the SWAVES Web site, <http://swaves.gsfc.nasa.gov/>.

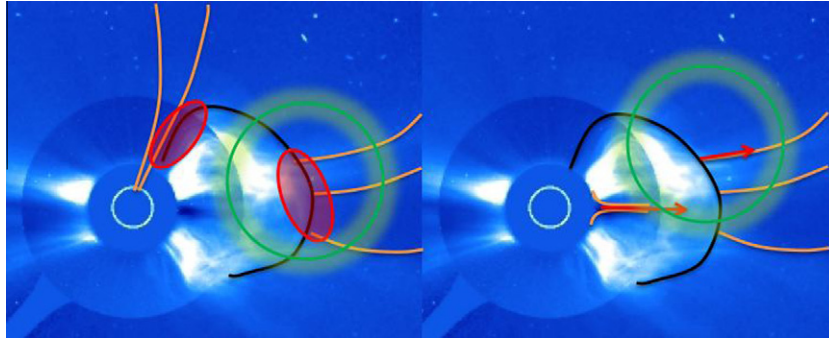


Fig. 2. Possible source regions for particle acceleration in the heliosphere. The image is of a CME observed by SOHO, and superposed lines indicate notional magnetic field lines (orange), shock waves (black), acceleration sites (red), and ROLSS angular resolution at 10 MHz (green). (a) Possible source regions of Type II bursts created by electrons accelerated near shock surfaces. These could be either at the nose of the shock (quasi-parallel) or on the flank (quasi-perpendicular). ROLSS will have the angular resolution sufficient to distinguish between these two scenarios. (b) Possible source regions of Type III bursts due to electron beams escaping along magnetic field lines into the heliosphere. These could be at the front of the CME or behind it in a reconnection region at its tail.

when successive CMEs leave the Sun within 24 h, as if CME interaction can produce enhanced particle acceleration (Gopalswamy et al., 2001, 2002; Richardson et al., 2003). Statistically associated with intense SEP events (Gopalswamy et al., 2004), this enhanced emission could result from more efficient acceleration due to changes in field topology, enhanced turbulence, or the direct interaction of the CMEs. The lack of radio imaging makes it difficult to determine the nature of the interaction.

The prime science mission for ROLSS is the particle acceleration and associated radio emission that occurs at many solar radii and at frequencies below 10 MHz. There is a long history of solar radio observations from the ground at higher frequencies, with a number of telescopes either currently or recently operational,² including the Clark Lake Radio Observatory (e.g., Sawant et al., 1982; Gopalswamy et al., 1987), the Culgoora Radioheliograph (e.g., Shanmugaraju et al., 2009; Kim et al., 2009), the Gauribidanur Radio Observatory (e.g., Ebenezer et al., 2001; Ramesh et al., 2008), the Green Bank Solar Radio Burst Spectrometer (e.g., Cho et al., 2007), the Bruny Island Radio Spectrometer (Erickson, 1997), the Murchison Wide-field Array (Oberoi et al., 2011), and the Low Frequency Array (LOFAR, Cairns, 2004). These ground-based observations both motivate and provide a useful complement to the observations that ROLSS will conduct.

2.2. Lunar ionosphere

The lunar ionosphere is a dynamic component of the tenuous atmosphere, and one that can have a significant effect on plans to use low frequency imaging arrays to

² Listed are notable telescopes that have been involved in solar radio research programs. There are also a number of telescopes used for radio wavelength monitoring of the Sun for space weather purposes by various civilian and military agencies around the world.

study solar and interplanetary radio sources. The existing data, mainly from dual-frequency radio occultation measurements, suggest that the density of free electrons is highly variable but can exceed 2000 cm^{-3} (Vyshlov, 1976; Vyshlov and Savich, 1978). The implied local plasma frequency is about 0.4 MHz.

The interpretation of these data is model dependent. Bauer (1996) concluded that the Luna data were consistent with no significant lunar ionosphere. However, ALSEP measurements during Apollo found a photo-electron layer near the surface with electron densities up to 10^4 cm^{-3} (Reasoner and O'Brien, 1972), implying a plasma frequency of 0.9 MHz. Such a high plasma frequency would affect radio observations at frequencies up to a few MHz, into the band proposed for ROLSS observations.

Below the plasma frequency, radio waves cannot propagate. Consequently, as ROLSS tracks solar radio bursts to lower frequencies, it will also be able to search for a lunar ionosphere. If a low frequency cutoff (e.g., around a few MHz) of the spectral index were observed, it would be an indication of lunar ionospheric absorption and would place a constraint on the total electron column of the lunar ionosphere.

2.3. Astrophysics

While not the prime mission of ROLSS, it may still be possible for the telescope to detect a few astronomical sources. Because the Sun is “bursty,” with occasions when it does not emit at all, ROLSS might also be able to be used to detect the strongest astronomical radio sources.

Low energy electrons are tied to a number of key issues in particle acceleration and source structure (Harris, 2005; Harris and Krawczynski, 2006). If nearby galaxies (e.g., M87, Biermann et al., 2001) are the sites of ultra-high energy particles, they must contain a low-energy reservoir of particles from which the particle acceleration is initiated. Estimates for the minimum electron energy range from

Table 1
Baseline technical specifications for the Radio Observatory on the Lunar Surface for Solar studies (ROLSS).

Parameter	Value	Comment
Wavelength (frequency)	30–300 m (1–10 MHz)	Matched to radio emission generated by particle acceleration in the inner heliosphere, Obtain spectra of Galactic and extragalactic sources at longest wavelengths, Probe lunar ionosphere, Operate longward of Earth's ionospheric cutoff
Angular resolution	2° (at 10 MHz)	Localize particle acceleration sites in CMEs and Type III solar bursts, Order of magnitude improvement
Bandwidth	100 kHz	Track (time-)evolution of particle acceleration
Temporal resolution	1 s	Track (time-)evolution of particle acceleration
Lifetime	1 yr	Obtain measurements during several solar rotations

$E < 50$ MeV to $E > 1$ GeV (Eilek and Hughes, 1991; Lesch and Birk, 1997). The limited measurements from the ground (Carilli et al., 1991; Lazio et al., 2006) suggest a cutoff near the low end of this range, but ground-based observations are limited to probing the electron energies $E > 0.5$ GeV, because of the Earth's ionospheric absorption. Observations at frequencies lower than those that can be detected from the ground are needed to verify these results. Low energy electrons also contain the bulk of the energy in a source and therefore constrain its total historical luminosity.

The baseline design described below has 16 antennas distributed over 3 arms, for a total of 48 antennas. The array should have a (1σ) sensitivity, in a 1-h integration at its higher frequencies, of about 10 Jy.³ By contrast, the stronger radio astronomical sources (e.g., 3C sources) should have flux densities approaching 500 Jy, with the very strongest having flux densities exceeding several thousand Janskys. While ROLSS will not be able to resolve these sources, it will still be able to determine their continuum flux densities. The extent to which their low frequency spectra flatten will constrain their low-energy electron populations.

3. Baseline design

The array consists of 3 arms arranged in a Y configuration, subject to local topographic constraints. Each arm is approximately 1000 m long, providing approximately 2° angular resolution at 30-m wavelength (10 MHz). Table 1 summarizes the technical specifications and the flow-down from the scientific requirements.

The arms themselves consist of a polyimide film on which electrically-short dipole antennas are deposited, and they hold the transmission system for sending the electrical signals back to the central electronics package (CEP), located at the intersection of the arms. The CEP performs the requisite filtering and digitization of the signals, then downlinks them to the ground for final imaging and scientific analysis. The array operates over the wavelength range 30–300 m (1–10 MHz), with a selectable, variable frequency sub-band being able to be placed anywhere within the operational wavelength range.

During the course of this concept study, we engaged the NASA/GSFC Instrument Design Laboratory (IDL) to study the ROLSS concept. We had a one-week study in 2008 May, followed by a one-day “ripple” study in 2008 June. We refer to the conclusions of or work during both of these studies to be output from the “IDL run.”

3.1. Science antennas

The ROLSS array consists of multiple science antennas. Each science antenna is a single polarization, electrically short dipole, deposited on a polyimide film; also deposited on the polyimide film are the transmission leads to a central electronics package. The polyimide film is flexible enough to be stored in a roll during transit and deployed directly on the lunar surface by unrolling.

The lunar regolith has a typical relative dielectric permittivity of 2–3 (for lunar soils), high resistivity, and a large skin depth at low radio frequencies. Consequently, it is possible for a low frequency radio antenna to operate when placed directly on the lunar surface. Our modeling of the electrical properties of polyimide film antennas indicates an optimum length of 14 m. The antenna resonant frequency will be near the high end of the ROLSS observing frequency range. At the low end of this range, the antenna will be electrically short and will have a small feed point resistance and high capacitive reactance. The radiation resistance, efficiency, and fractional bandwidth will all be very small, thereby reducing the sensitivity. Fortunately, the background sky brightness increases at lower frequencies; this partly compensates for the reduced sensitivity.

The baseline design has 16 antennas per arm spaced logarithmically in order to provide a range of Fourier spacings for good imaging. The nominal topology is a wide dipole, with an approximately 1-m width, which helps provide a broad wavelength response. Each of the dipoles is connected to the CEP at the end of the polyimide film by transmission lines deposited on the film.

We have conducted two tests of this ROLSS antenna concept. The first test was a comparison of the feed point impedance of a polyimide-film based antenna lying directly on the ground (Fig. 3). This test was conducted to verify that our simulations of the antenna concept were accurate and did not involve extrapolations of modeling software into a regime of parameter space for which they are not

³ 1 Jy = 10^{-26} W m⁻² Hz⁻¹.

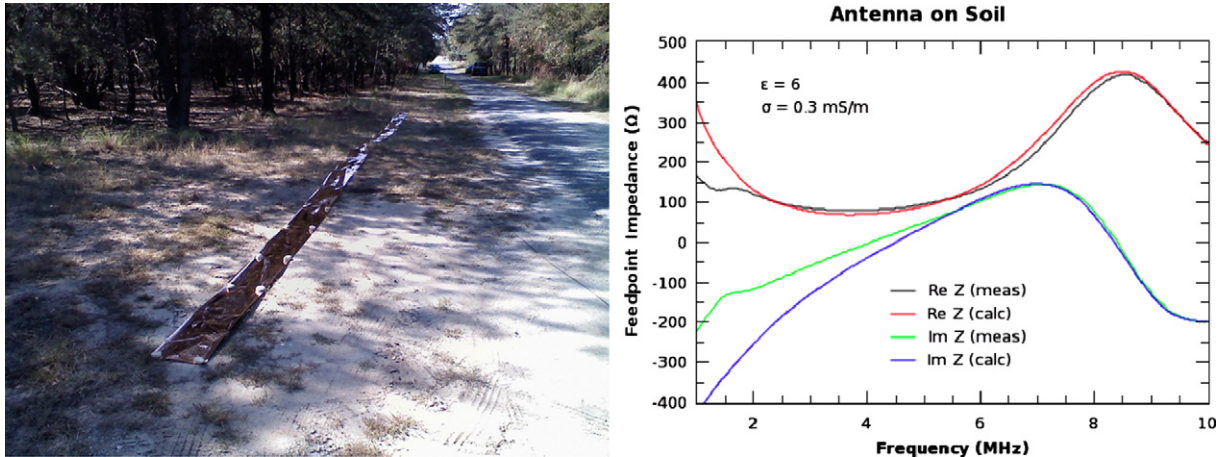


Fig. 3. (Left) A picture of the proof-of-concept antenna deployed at NASA/GSFC. Rocks had to be placed along its edges in order to prevent the antenna from blowing away in the wind. (Right) A comparison of the measured impedances (real, black; imaginary, green) with simulations, assuming a canonical value for the dielectric constant of sandy ground (real, red; imaginary blue).

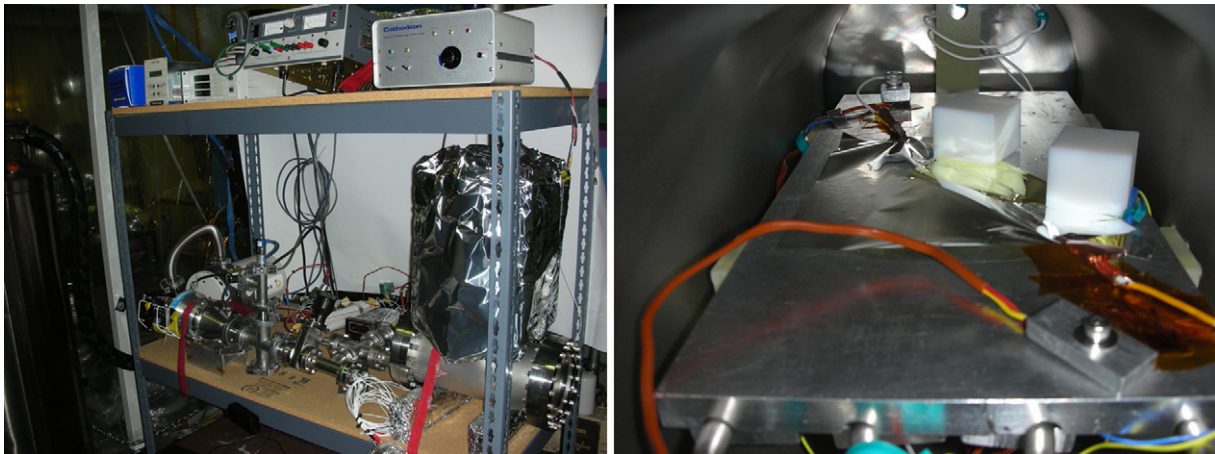


Fig. 4. (Left) The primary thermal-vac test setup for ROLSS testing at the Astrophysics Research Lab (ARL) of Center for Astrophysics and Space Astronomy at the University of Colorado. (Right) The interior of the chamber showing the 10 cm × 10 cm polyimide film test sample.

valid. The test consisted of a single antenna, two 8-m long segments each 30.5 cm wide, and composed of a 25 μm -thick Kapton™ film⁴ with a 5 μm -thick Cu layer deposited on it. The feed point impedance was measured via a network analyzer, and the test was conducted at NASA/GSFC. The test scenario was simulated using the CST Microwave Studio 3D package, with various estimates of the ground characteristics at the NASA/GSFC site. The simulations were not complete, in that they did not attempt to model the small air gaps underneath the antenna where it did not rest flat on the ground, and the ground was only modeled to a depth of 15 m in order to maintain reasonable computation times. Nonetheless, the agreement between simulation and measurement is considerable.

⁴ This film was not space-rated, as we judged a space rating as not required for testing this aspect of the antenna concept.

The second test consisted of exposing a polyimide film sample to a simulated lunar environment (Fig. 4). We constructed a small thermal vacuum chamber with an interior UV lamp. The chamber contained a platform on which a polyimide film sample could rest, and the temperature of the platform could be changed from $-150\text{ }^{\circ}\text{C}$ to $+100\text{ }^{\circ}\text{C}$.

Two space-rated polyimide film samples were acquired from ManTech SRS. Each was a 10 cm diameter circular sample, 8 μm in thickness, with a silver coating on one side. Prior to exposing one of these samples to the simulated lunar environment, a number of preliminary tests were conducted. A bake-out test on one of the samples showed no evidence of outgassing. During this test, the polyimide film was folded. There was no evidence of stiction for the film-film contact, but there was evidence for stiction and removal of the silver coating for silver-silver contact. This outcome is in agreement with experience from the Hubble Space Telescope in which metal-metal contact could lead to

stiction and removal of the metal. However, stiction should present no significant problems for ROLSS antenna arms because, when rolled, there should be only film–film or film–metal contact.

The test plan focused on the large temperature changes and UV exposure encountered over the course of a year. The test film was exposed to a total of 12 cycles over the course of 24 days, from hot (+100 °C) to cold (−150 °C) and back to hot, at the maximum rate possible with the temperature control system, with the sample also exposed to a deuterium lamp while in the hot cycle. After the simulated year exposure to lunar conditions, the film sample was evaluated for tensile strength, electrical conductivity, and flexibility. No change in the film’s properties, typically to 5% precision or better, was found.

3.2. Transmission lines

The transmission lines carry the signals from the antennas to the CEP. Like the antennas, they consist of a conductor deposited on the polyimide film; they are formed on the same polyimide film as the antennas. Each transmission line is a coplanar waveguide structure (6.2 mm wide). Simulations, conducted as part of the IDL run (Fig. 5), indicate that the gap between the lines reduces cross coupling and suggest that the lines should be placed symmetrically to reduce antenna pattern distortions. These simulations suggest that approximately 25 dB of signal loss will occur on the longest transmission lines. It is likely that the transmission lines will need a flash coating of polyimide film (or other non-conductor) to minimize the risks of short circuits.

The width of the transmission lines is determined in part by the requirement of mitigating micrometeorite damage. During the IDL run, estimates of the micrometeorite damage were determined by scaling from experience with the Hubble Space Telescope (HST) Wide Field/Planetary Camera (WF/PC) radiator. The estimated bombardment rate at the Moon’s surface is $4.9 \text{ m}^{-2} \text{ yr}^{-1}$ for impacts producing craters up to 1 mm wide. Larger craters are sufficiently rare that none were seen in a 3.6-yr exposure. The longest transmission lines are likely to receive a few impacts per year (~ 3), but none are likely to be so large that the transmission line will be completely severed.

In the original ROLSS concept, the signals would be transmitted directly to the CEP from the antennas, where

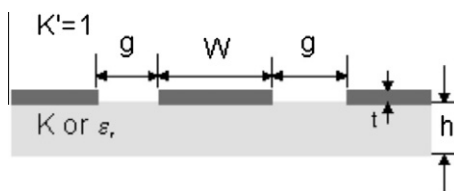


Fig. 5. Cross section of the transmission line. The light gray indicates the substrate. The dark gray shows the deposited metal. Nominal dimensions are a conductor width of $W = 2 \text{ mm}$, a gap of $g = 1 \text{ mm}$, and thickness of $t = 70 \text{ }\mu\text{m}$. (Figure from IDL run.)

all conditioning and processing of the signal would happen. As the concept study advanced, and with subsequent work, it appears likely that there would have to be pre-amplifiers at the antenna to overcome the losses along the transmission lines (Jones, 2011). A detailed study of how and where preamplifiers would be mated to the antennas has not been performed. However, there are commercially available electronic components (e.g., resistors) that are products that use polyimide film as a substrate. Thus, having small pre-amplifiers at each antenna is conceptually possible. A key requirement, of course, is that the pre-amplifiers do not vitiate the capability to roll up the polyimide film.

3.3. Science antenna receivers

ROLSS measurements will be optimized for observations of the region of space from approximately $2\text{--}10 R_{\odot}$. Over this range of distances, densities vary by a factor of 100, and plasma frequencies by a factor of 10. Consequently, the frequency bandwidth for a given image needs to be a small fraction of the central “image” frequency, in order to permit separation of time evolution from spatial distribution for the propagating radio sources. Table 2 summarizes the receiver specifications and downlink requirements.

The solar radio bursts identified as the primary target of ROLSS have a considerable range of intensities and would be at or above the “Galactic background.” From 1 to 10 MHz, this background level corresponds to a flux density of $10^{19} \text{ W m}^{-2} \text{ Hz}^{-1}$; some intense Type III radio burst peak flux densities will exceed this background by 4 orders of magnitude or more, and the major solar bursts are substantially more intense than the terrestrial RFI, which is typically less than 10 times the flux density of the Galactic background at the distance of the Moon.

Although the ROLSS frequency range of interest corresponds to the Wind/Waves RAD2 range, the ROLSS receiver design will be quite different. The RAD2 superheterodyne receivers cover the frequency range from 1 to 14 MHz with 256 selectable frequencies. In swept frequency mode, the fastest sweep has each successive frequency being sampled for 63 ms; the signal is filtered to reduce noise and to define a single representative level of the signal for that sampling interval. This result is obviously different than that desired for aperture synthesis. In the case of ROLSS, the current intention is to telemeter the sampled waveform data to Earth.

In an attempt to minimize the number of ROLSS receiver components, it is tempting to think of a single wide-band digital receiver for each antenna. The signals from the antennas would (after preamplification) be fed directly to analog-digital converters (ADC) for digitization, facilitating subsequent processing. For observing frequencies up to 10 MHz, the desired ADC is readily available in commercial form. Issues relating to available power, radiation tolerance, and function in the lunar environment need to be addressed further.

Table 2
ROLSS receiver specifications.

Given	Number of frequency channels	10 log-spaced (swept-freq.)
	Frequency range	1–10 MHz
	Instantaneous bandwidth	2% of central frequency
	Number of antennas	48 total (on 3 arms)
	Number of dipoles	1 per antenna location
	Pre-correlation sampling (bits)	2
	Data to downlink	Rate (assuming continuous d/l)
		1.96 MB/s
Total daily data volume		170 GB

Consideration of the terrestrial RFI entering the wide-band front end is equally critical. Roughly half of the band is contaminated by terrestrial signals. Accepting all of this noise in the first stage of the digital receiver will significantly increase the noise floor, and will make it difficult to study weak solar events. For example, if a moderately intense solar burst produces a peak-to-peak voltage of about $10 \text{ nV Hz}^{-1/2}$ at the antenna feed-points at a frequency of 10 MHz, then the signal at the receiver input would be less than $1 \text{ } \mu\text{V Hz}^{-1/2}$ with a preamplification gain of 20 dB. (Two amplification stages might be required to obtain this amount of gain.) For a 2% bandwidth of 200 kHz, the corresponding voltage would be about 0.4 mV (peak-to-peak), a signal that would be measurable by an ADC with 2 V (peak-to-peak) range and an effective number of bits (ENOB) of 12. This would require a 16-bit ADC, operating at greater than $20 \text{ Msamples s}^{-1}$. Alternately, an automatic gain control (AGC) could be used with fewer bits to be converted, but there is a limit to the amount of gain that can be realized. The minimum requirement is that the weakest measurable, in-band signal flips the least significant bit in a correlated sense, which seems relatively easy for the solar burst under consideration.

If we consider that the noise signal from terrestrial RFI will be about one-tenth the voltage of our weak solar event, but spread across roughly half of the 1–10 MHz full bandwidth, the problem is clear. The noise floor produced by the RFI will be about 0.3 mV at the receiver inputs, making the detection of the 200 kHz bandwidth signal from the solar burst at 10 MHz challenging. Either ROLSS will be restricted to the more intense solar events or a receiver architecture with narrow-band sampling is required, not unlike the super-heterodyne receivers. This in turn means that additional analog components must be implemented in a manner that can survive the lunar environment. As such, the ROLSS receivers, with one receiver per antenna required, becomes a “tall pole” in the development strategy.

The specifics of the receiver design for ROLSS require a system that is resistant to the lunar thermal environment and ideally capable of avoiding terrestrial RFI by frequency agility and other techniques. Attention to real-time band-pass selection to permit selection of frequencies

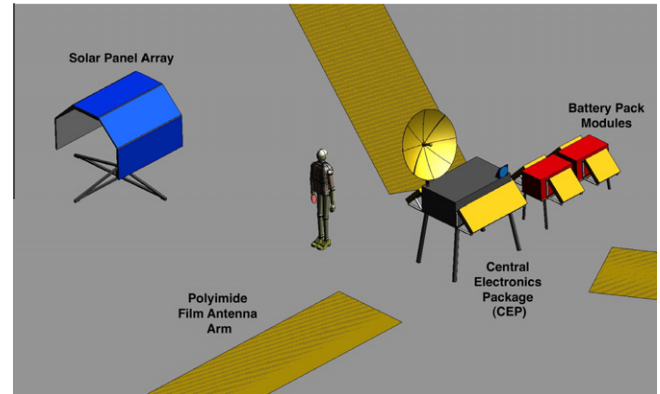


Fig. 6. Illustration of the central electronics package (CEP) and deployed ROLSS system. Shown are the arms without the connection to the CEP. The CEP sits near the center of the figure with the downlink antenna on top. The solar panel array is near the top left, again without the cabling to the CEP shown. To the right of the CEP are two optional battery modules. (Figure from IDL run.)

where RFI is not occurring will facilitate observing over the entire frequency range.

3.4. Central electronics package (CEP)

The CEP houses all of the science antenna receivers, data acquisition hardware, power supply electronics, data and telemetry communications electronics, and the thermal management system for these components. The CEP is designed to be carried in a standard lunar lander carrier, having approximate dimensions of $2.5 \text{ m} \times 1 \text{ m}$. When deployed (Fig. 6), the CEP stands approximately 1 m above the lunar surface in order that the thermal management system (see below) is not subject to dust contamination.

3.5. Telemetry and data downlink

Telemetry and commanding would be handled by an S-band uplink. A nominal configuration for the ground station has a 9-m diameter or larger antenna at a site such as GSFC Wallops. The ROLSS CEP would contain an S-band transceiver, which could also be used for data downlink in emergency situations.

Data downlink would be handled by a Ka-band system. The ROLSS CEP would host a 0.6-m diameter gimbaled antenna. A gimbaled antenna is necessary because the beamwidth of a 0.6-m is smaller than the apparent motion of the Earth in the lunar sky due to lunar librations. An antenna of diameter approximately 0.35 m would not require a gimbal but would require a much larger transmitter power in order to meet the link budget margin for reasonable ground-site antenna diameters.

The Ka band allows for an 80 Mb s^{-1} data rate, higher than can be achieved in the X band allocation for spacecraft downlinks, but there is a higher risk of data loss due to rain at the ground site. During the IDL Run, the

fraction of time that the downlink margin would not be suitable was estimated to be less than 2% for a ground site such as White Sands. JPL has procured and conducted initial testing of a 12-m diameter antenna that operates to Ka band, and, on the ROLSS time scale, antennas with 12-m diameter are assumed to be available.

The gimbals would have to be protected from lunar dust contamination. A “bellows” covering the gimbals is a low mass and relatively small means of doing so. An alternate approach, likely to be lower mass but much larger, would be a radome covering the entire antenna.

We also considered a phased array as a downlink option. A phased array has the attractive feature of requiring no moving parts, and there are designs under development for phased arrays that could “self-phase” on a carrier signal from Earth. Current extrapolations suggest that the phased array would not be substantially lower mass than a parabolic antenna and would require as much as 300 W of power, which we judge to be too large. Future optimization of the design might enable this power budget to be reduced substantially, however.

3.6. Power generation

The baseline ROLSS design assumes a solar panel assembly for power generation. Multiple load profiles were generated during the IDL run, with the final load profile suggesting that an average 125 W load (peak 167 W load) could be generated by solar panels (Table 3). Only daytime operation is assumed, per the prime science mission.

Also suggested during the IDL run, but not considered in any depth, was the possibility of micro-batteries, if power is needed during the night. The use of micro-batteries would spread thermal losses as well as reduce cable length and mass, with a likely increase in reliability.

Discussions with personnel at NASA/Glenn Research Center suggest that radioisotope thermal generators (RTGs) with suitable power production and lower mass than the equivalent solar panel array could be developed. Detailed consideration of such RTGs was beyond the scope of this study and were explicitly not considered in our IDL run.

3.7. Thermal management

The antenna arms are entirely passive and require no thermal management. For operation over multiple lunar day-night cycles, the polyimide film and deposited antennas and transmission lines should have coefficients of

thermal expansion that are as similar as possible. If the coefficients of thermal expansion are significantly different, connections could be disrupted by thermally-induced shear between the metal and polyimide film.

The CEP is equipped with a set of radiators in order to maintain the internal electronics at a temperature below their assumed maximum operating temperature (80 °C) during the lunar day. These radiators are equipped with thermal louvers, outfitted with actuators that sense radiator temperature and rotate thin aluminum blades to open or closed positions. When open, the louvers allow the radiators to dissipate heat. The actuators do not require any power and operate automatically, opening as the CEP is exposed to sunlight and warms during the beginning of the day and closing as the CEP cools at the beginning of the night. The radiators and louvers are covered with a sunshield. It serves the dual purpose of keeping the Sun from direct exposure onto the radiator as well as reducing dust contamination. Thermal radiators with louvers and sunshields have a long spaceflight history (30+ yr) and high reliability, with some models still operational 20 yr after launch.

As discussed further in Section 3.9, ROLSS will operate only during day. In this concept design, ROLSS carries a sufficient number of batteries to maintain the CEP at a survival temperature for any electronic components and the batteries themselves. Radio telescope receivers are operated commonly in cryogenic containers, cooled to temperatures well below those obtained on the lunar surface. However, not all electronics and the current generation of batteries cannot withstand these temperatures. Thus, small heaters would be used to maintain these components at the required temperature.

3.8. Configuration and imaging

The Y configuration for ROLSS was chosen for two reasons: (1) It enables easy deployment of the polyimide-film based antennas; and (2) It provides for relatively high dynamic range snapshot imaging. The latter point distinguishes lunar imaging from terrestrial imaging. Earth-rotation synthesis often used by ground-based telescopes exploits the rotation rate of the Earth. In contrast, the lunar rotation rate is over 20 times slower. Further, the dynamic processes of the Sun require that the images be produced on time scales of about a few seconds, far too rapidly to use lunar-rotation synthesis.

Fig. 7 shows a nominal layout of 16 science antennas along the arms. Standard radio astronomical software within the Astronomical Image Processing Software (AIPS) package of the National Radio Astronomy Observatory (NRAO) was used to simulate the instantaneous or “snapshot” point spread function (PSF) or “beam” of the ROLSS array, assuming 16 antennas on each arm and a logarithmic spacing along the arm. The 6-arm “star” pattern of the beam in Fig. 7 reflects the Y shape of the ROLSS array.

Table 3
ROLSS power profile.

Power profile	Solar array
125 W (average)	5 × 0.48 m ² panels
167 W (peak)	Panels form 5 sides of 8-sided figure for uniform solar illumination during the day

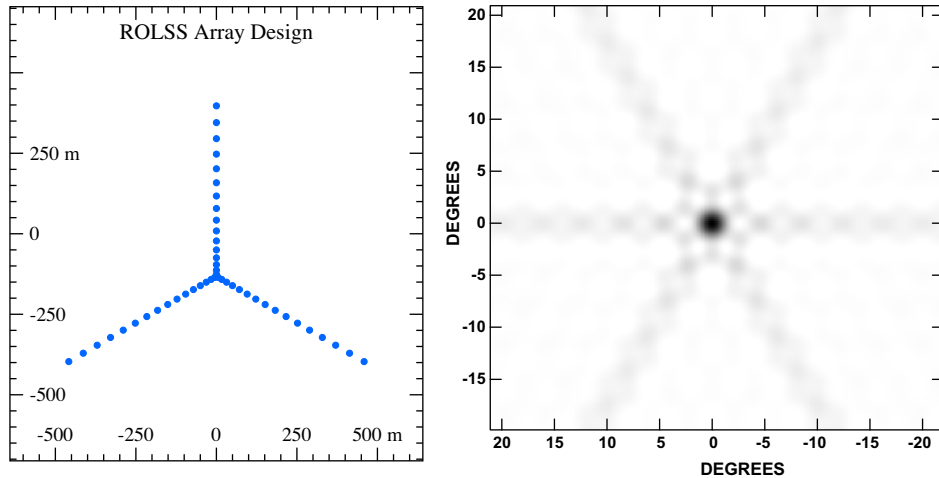


Fig. 7. (Left) Nominal science antenna distribution along the antenna arms. (Right) The resulting point-spread function (“beam”) for a snapshot image. The maximum sidelobe is at -5.9 dB, and the rms sidelobe level is -15 dB.

The dynamic range in the beam—defined as the ratio between the peak and the rms level—is 15 dB. This dynamic range is consistent with that expected on the basis of a simple analysis that the rms level in an interferometric image should be of order $1/N$ if the array consists of N antennas. For $N \sim 50$ ($\sim 16 \times 3$), the expected rms level is of order 2% of the peak.

We investigated both different numbers of antennas as well as their distribution along the arms, characterized by a power-law radial scaling as $r^{-\alpha}$. For reasonable number of science antennas per arm (12–20) and power law exponents comparable to those for ground-based imaging telescopes (1–2), no significant differences were seen in the amplitude of sidelobes. The positions of the sidelobes do vary, but as the Sun is expected to be the strongest source in the field of view, any other celestial sources that the

sidelobes intersect will not corrupt the image by any substantive amount.

Fig. 8 illustrates the imaging capabilities of ROLSS. We used the model of Schmidt and Gopalswamy (2008), scaled to a frequency of 10 MHz, to produce a “truth” image of a CME, as an illustration of the kind of target for ROLSS. It is apparent that the front and back sides of the CME can be distinguished. A modest amount of deconvolution (CLEAN) of the simulated image was performed, and additional signal processing could likely improve the image further. Nonetheless, even this simple simulation demonstrates that the current design for ROLSS would be capable of meeting the science requirements, as source regions for radio emission (i.e., particle acceleration) around a CME could be distinguished (viz. Fig. 2).

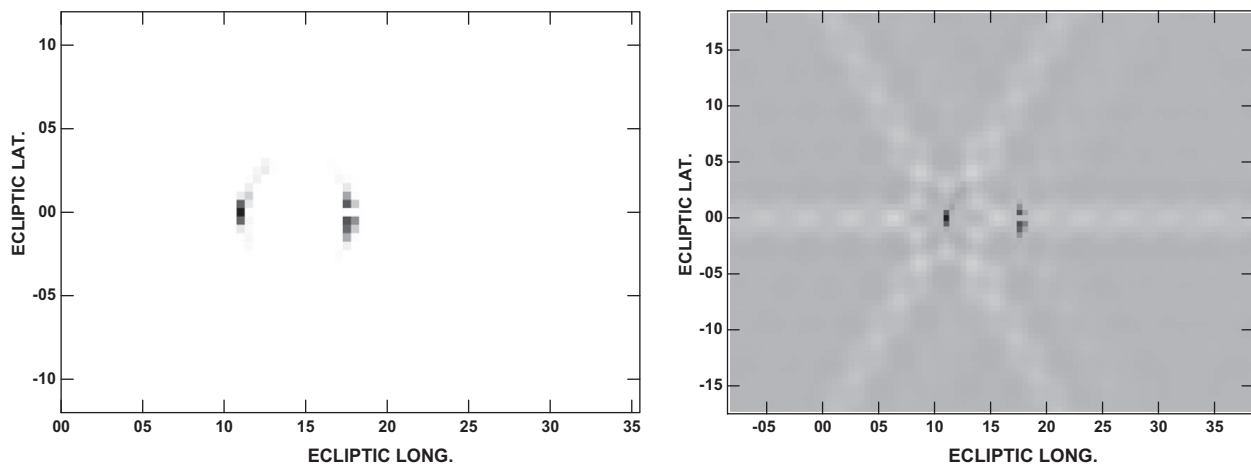


Fig. 8. (Left) A model CME at 10 MHz, scaled from those developed by Schmidt and Gopalswamy (2008). Illustrated is a circular CME soon after lift-off from the Sun. The Sun is not shown in this model, but is immediately to the left of the CME. (Right) The imaged CME. The front and back of the CME are clearly distinguished, even though residual beam effects are also apparent. Only a modest amount of deconvolution (CLEAN) was performed on this image, and additional post-processing would likely improve the dynamic range further. This figure demonstrates that the ROLSS concept would be capable of satisfying the science requirements.

These simulations of the beam have not taken into account the difference between the radii of the Earth and the Moon. Traditionally, ground-based radio interferometers have used a two-dimensional fast Fourier transform (FFT). Implicit in the use of a two-dimensional FFT is that the field of view is restricted. Perley (1989) discusses how the use of a two-dimensional FFT is equivalent to assuming the array to be co-planar and describes a criterion by which the coplanarity of the array can be assessed ($\theta_{\max} \approx \sqrt{\theta_{\text{beam}}}$, for a synthesized beam width θ_{beam}). For ROLSS, the synthesized beam is $\theta_{\text{beam}} \approx 0.03$ ($\approx 2^\circ$), implying that the maximum field of view over which two-dimensional FFT imaging is satisfied is about 10° (0.17 radians). Thus, the difference between the radius of the Earth and Moon only needs to be considered when imaging fields of view much larger than 10° .

3.9. Operations

The prime science mission is solar observations. Consequently, ROLSS would acquire data only during the lunar day, with no nighttime operations planned. The design mission lifetime is 1 yr, based on the science requirement to acquire data over multiple solar rotations. An extended mission of up to 5 yr would sample a significant fraction of a solar (magnetic) cycle.

After emerging from nighttime, there would be a power-up and self-health check cycle. Data acquisition would occur on a continuing basis, with the data written to a solid-state recorder in the CEP. The priority of the data would be calculated on-board, with the continual operation of the solid-state recorder allowing for the overwriting of data. Upon ground command, data would be down-linked, with an approximate volume of 20 h of data over aggregate of 6 h. Before entering night, equipment would be powered down and a final data downlink would be performed.

4. Siting and deployment

The prime science mission for ROLSS is solar observations, which favors an equatorial site (Fig. 9). A polar site would require that one or more arms of ROLSS be longer than the nominal 1000 m length in order to compensate for the foreshortening of the array and maintain the same angular resolution. Assuming a completely spherical surface, the foreshortening scales as $\sec \beta$ for a lunar latitude β . As an illustration, a polar site at $\beta \approx 85^\circ$ would require that one or more arms be potentially 11 times longer (11 km) to maintain the same angular resolution. This foreshortening potentially could be mitigated by deployment that takes advantage of local topography, e.g., the side of an equatorially-facing hill, however, such considerations are clearly dependent on the characteristics of any polar sites.

With respect to equatorial sites, there are no additional requirements implied by the prime science mission.

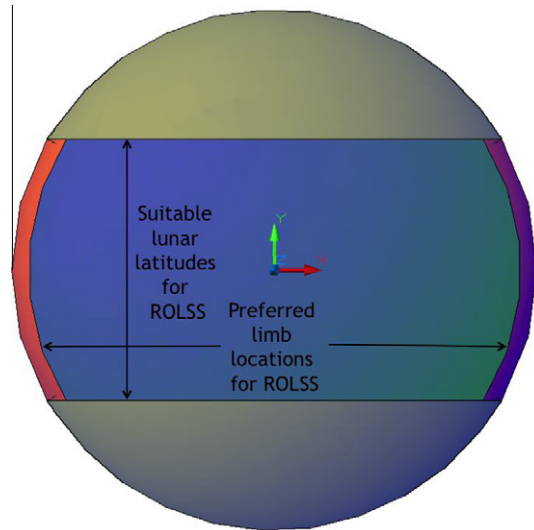


Fig. 9. Illustration of suitable ROLSS siting locations on the (near side of) Moon (blue-green shaded region). The orange and purple shaded areas indicate equatorial regions ($\pm 30^\circ$ latitude) on the limb of the Moon. Siting on the limb of the Moon has the beneficial effect of placing the Earth in a naturally low sensitivity portion of the science antennas' power patterns, reducing the impact of terrestrial radio emissions on ROLSS science measurements. (Figure from IDL run.)

However, a site on the limb would offer benefits for the instrument design. The nominal antenna topology is a dipole laying flat on the surface, which has a natural decrease in sensitivity at large zenith angles. An equatorial site on the limb (Fig. 9) would place the Earth toward the horizon, where the dipole sensitivities would be decreasing. Thus, human-generated RFI would have an additional modest suppression factor. In turn, this additional suppression could enable a slightly more simple receiver design.

A site on the near side is sufficient for the prime science mission. The Sun illuminates both the near and far sides of the Moon, during different portions of the orbit. A near side site offers the benefit of easier access and easier communications, and, since ROLSS' operational frequencies are below the typical terrestrial ionospheric cutoff frequency, the array would be at least partially protected from terrestrial transmissions.

The site itself should be of relatively low relief topography (e.g., the surface of a mare vs. the highlands). We emphasize that the entire site does not have to be flat as the fraction of the area occupied by the antenna arms is relatively small—for a circular area with a radius of 500 m, the antenna arms occupy only 0.3% of the total area. Further, there is no requirement on the absolute orientation of the arms. Rotating the arms about the center of the array merely rotates the beam pattern on the sky (Figs. 7 and 8).

The *relative* orientation of the arms is required to be $120^\circ \pm 6^\circ$, with the error determined by requiring that the nominal antenna position not vary by more than 1 wavelength at the extreme end of an arm. This level of alignment was demonstrated during the Apollo missions.

Only modest requirements are set on the smoothness of the antenna arm locations. The shortest operational

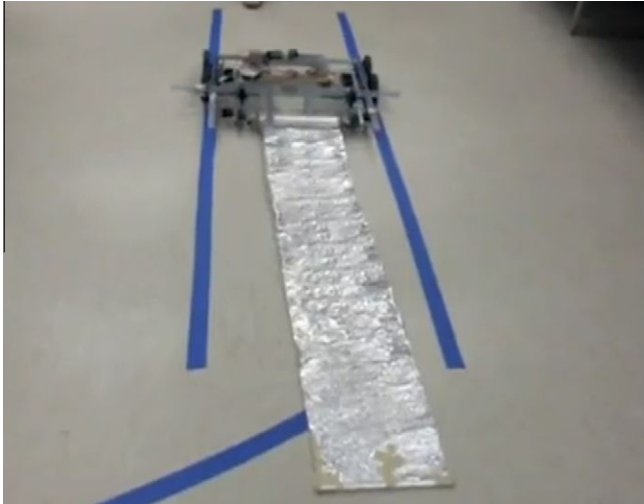


Fig. 10. A telerobotically operated rover constructed as part of a high school class project at the Thomas Jefferson High School for Science and Technology. Shown is one of the frames of a movie in which the rover is maneuvered to a deployment site, then deploys aluminum foil. The aluminum foil is used a proxy for polyimide film.

wavelength for ROLSS would be $\lambda = 30$ m, and an individual science antenna would be 15 m in length. Requiring that the antenna shapes are not distorted by more than $\lambda/10$ implies that deployment requires linear extents of order 1000 m with rocks not larger than about 3 m in size along the intended antenna arm positions. We assume that on the timescale of likely deployment for ROLSS that any site will have better than meter-scale resolution images available (post-Lunar Reconnaissance Orbiter).

Deployment itself could be done completely robotically, by astronauts on a crewed rover, or with a mix of these two modes. During the IDL run, astronaut deployment from a crewed rover was assumed. The Apollo rovers traversed longer distances than the size of ROLSS; the only significant requirement on a crewed rover is that it be able to move slowly enough to enable the polyimide film to spool out without tearing. With respect to astronaut involvement during deployment, the ROLSS array is low risk to astronauts. The array itself is simple, with no moving parts or sharp edges, once deployed, and the array is intended to operate autonomously after deployment. There may be a potential risk with charging of the solar arrays during deployment. However, the procedures for handling solar arrays are well developed, and other lunar missions are also likely to require solar arrays for power.

A completely robotic deployment would allow for ROLSS to be deployed prior to any human missions. There are multiple possible concepts that would have to be explored in more depth and optimized. For instance, the mission could be deployed by a single rover, which would be responsible for deploying the arms and then returning to the center of the array, attaching itself to the arms, and hosting the CEP. Alternately, multiple “disposable” rovers could deploy the arms from the lander, with the

CEP stationed on the lander. This latter possibility is conceptually similar to the Mars Pathfinder mission that consisted of a lander and the *Sojourner* rover, except that the *Sojourner* rover did not maintain a physical connection to the lander. Fig. 10 illustrates that polyimide film deployment by a rover, while presenting various challenges, should nonetheless be possible.⁵ Scaling from JPL’s ATHLETE rover, a ROLSS rover could be designed to carry and deploy several tens of kilograms of antenna mass.

5. Technology roadmap

In this section, we summarize a technology roadmap for ROLSS (Table 4). We emphasize that while our focus here is on the ROLSS, many of these technologies have a much broader applicability than just for the ROLSS. Further, the underlying concept of radio interferometry has a significant Earth-based experience base (50 yr) and many of the key technical challenges relevant to the ROLSS relate to enabling a sufficient collecting area on the Moon. For the ROLSS mission, technology challenges are more engineering than technology investment, with a few key exceptions. Sustained investments over the coming decade are likely to mature a number of major technology areas satisfactorily.

5.1. Science antennas

Low-frequency radio astronomical detectors have a long history, as many of the first radio astronomy measurements were made at frequencies not too much different than those targeted by ROLSS. A prototype antenna for the ground-based Long Wavelength Array (LWA) operating in the frequency range $\nu = 20\text{--}80$ MHz ($\lambda = 4\text{--}15$ m) has been fabricated, with a modest amount of testing below 10 MHz. The final LWA antenna design has manufacturability as a criterion, but it will not be significantly smaller. Its mass is lower, but remains unacceptably high for a space mission, and the LWA antennas need to tolerate only modest changes in temperature. The antenna designs for all of the other ground-based telescopes suffer similar shortcomings with respect to operation in the lunar environment.

Dipoles imprinted on polyimide film offer promise, but significant simulation and prototyping work remains. As part of the ROLSS study, initial modeling, thermal-vacuum chambers tests, and field tests have been conducted. However, the scope of those studies has been too short to enable a sufficiently in-depth exploration of the parameter space for ROLSS antennas. Activities over the next decade would include

- Continued modeling of the radio frequency (RF) performance of the dipoles and transmission lines;

⁵ This figure is one frame of a movie. The full movie is available at <http://www.youtube.com/watch?v=O9Q9y-rZanU>

Table 4
Technology status and development needed for ROLSS.

Technology	Sub-system	Required technology (baseline)	Required TRL 6 product	Heritage	Comments
Science Antennas	Science Antennas	Good RF performance, structural stability	Efficient short antenna design	Near-future ground arrays	ROLSS tests provide initial support for dipole-on-film approach
Ultra-low power electronics (ULP)	Receivers, station electronics, correlator	ADCs, FPGAs, or similar boards implemented with ULP technology	Lunar-qualified ADCs, FPGAs	NASA ST5 Reed-Solomon encoders, GeoSTAR correlator	Relevance to many NASA missions, significant NASA experience, possible other Governmental synergies
Batteries	Power	Survival temperatures comparable to lunar temperature extremes	Lunar-qualified battery	Spaceflight batteries	Relevance to many other NASA missions
Rovers (either robotic or crewed)	Deployment	Autonomous navigation and antenna deployment up to 1 km from landing site	Lunar-qualified rover	Mars rovers, ATHLETE development	Relevance to both human- and robotic lunar exploration, significant JPL rover experience, possible DARPA synergies

- Verifying the RF performance of proof-of-concept models;
- Verifying that proof-of-concept models can withstand the lunar environment, including the thermal and UV exposure; and
- Demonstrate interferometric fringes using proof-of-concept models on targets such as the Sun, Cas A, or Cyg A, all of which have been observed with LWA hardware.

Based on experience from the antenna development for the LWA and similar ground-based arrays, 3 yr is the requisite amount of time to take an antenna concept from simulation to initial verification. Some of these tests could be conducted in a manner that both leverages existing low-frequency interferometers as well as using these instruments a means of quantifying its performance. Possible test sites include the LWA site in New Mexico, the Precision Array to Probe the Epoch of Reionization (PAPER) site in Green Bank, WV, or the Goddard Decametric Radio Observatory (GDRO) site in Maryland.

5.2. Ultra-low power electronics

Ultra-low power electronics (ULP) offers the promise of reducing the power requirements of ROLSS electronic components by an order of magnitude or more. Significant flight heritage exists for receivers at frequencies comparable to those envisioned for ROLSS (e.g., the radio instruments on the NASA Wind, *Cassini*, and STEREO spacecraft; the NRL SCITRIS instrument; and the Los Alamos FORTE satellite). Thus, the focus for the next decade should be on developing ULP technology and engineering receivers that could utilize it.

ULP technology, such as the CMOS Ultra-Low Power Radiation Tolerant (CULPRiT) technology, has been demonstrated on the NASA ST5 spacecraft in 2006 March. The CULPRiT technology lowers the logic voltage of an integrated circuit to the level of 0.5 V, and thus greatly reduces

the required power. Compared to a 5 V component, the power saving would be 100:1. On ST5, the CULPRiT part was a Reed-Solomon encoder which adds redundant bits to the data stream to protect them in the noisy communication channel. Two Reed-Solomon encoders were implemented in parallel: one with 5 V logic, the other 0.5 V logic. A comparison of the two encoders detected no error over the 90-day mission (over 300 million telemetry frames). Also relevant to ROLSS is the fabrication of a correlator for the Lightweight Rainfall Radiometer.

Activities over the next decade would include

- Design and fabrication of ULP chips such as field programmable gate arrays (FPGAs) and subsystem communication interfaces;
- Designs for interfacing ULP and traditional CMOS parts such as high-density memories;
- Designs for integrated analog and digital ULP circuits in the same chip;
- Development of a power supply with 0.5 V output at several hundred milliamperes of current is needed; and
- Fabrication of mixed ULP and non-ULP circuits followed by the demonstration that there are no unintended electrical interactions between them.

5.3. Batteries

The nominal ROLSS concept carries batteries within the CEP for power. However, a sufficient number of batteries must be carried to provide power during the lunar night in order to keep the temperature of the batteries within their survival range. Expanding this survival range would reduce the number of batteries for the mission, and therefore its total mass.

We expect that there will be continued investments in battery technology, both by Government agencies and commercial firms, for a variety of applications (e.g., electric and hybrid automobiles). Many of these applications might

not require expanding the operational and survival temperature ranges for batteries, though other lunar missions would clearly benefit, as might missions to the outer solar system.

5.4. Rovers

While the ROLSS concept could be deployed either via astronauts or entirely robotically, a rover will be a key component of either deployment scenario. A primary requirement for robotic rovers intended for deployment of ROLSS components is low mass for their mobility and manipulation capabilities; a crewed rover must have the capability of having a suitable deployment attachment.

Activities over the next decade would focus either on construction of a prototype deployment mechanism for attachment to a crewed rover or on determining a rover mass estimate for a completely robotic rover. In the former case, a key aspect will be the interface between the crewed rover and the deployment mechanism itself. In the latter case, a full-scale (if not flight qualifiable) rover that has demonstrated the needed level of mobility, stability, and dexterity should be constructed. In either case, crewed or robotic deployment, it is essential to demonstrate that deployment of polyimide film-based antennas is possible, using a to-scale model with a full test payload.

6. Conclusions

We have described the Radio Observatory on the Lunar Surface for Solar studies (ROLSS), an imaging radio interferometer designed to be deployed on the lunar surface, either during a sortie mission or completely robotically, and having a prime science mission of probing particle acceleration in the inner heliosphere.

Key science for ROLSS includes (i) Resolving the relevant geometry (quasi-parallel vs. quasi-perpendicular) at which particle acceleration occurs as coronal mass ejection (CME) shock fronts; (ii) Resolving the site of magnetic reconnection and electron acceleration near CMEs (front vs. back) associated with complex Type III (or Type III-L) radio bursts and proton solar energetic particle (SEP) events; and (iii) Resolving the nature of the interaction between successive CMEs and unusually intense radio emission. Secondary science includes probing the lunar ionosphere by searching for absorption of solar radio emission at ROLSS' lowest operational frequencies and constraining the nature of particle acceleration in astrophysical sources by determining their integrated continuum spectra.

The baseline design consists of 3 arms arranged in a Y configuration. Each arm is 1000 m long, providing the required 2° angular resolution at 30-m wavelength (10 MHz). We performed simulations of the imaging performance of this nominal array design, using model CME images. The baseline design provides sufficient imaging fidelity to meet the prime science mission of (relatively)

high angular resolution imaging of CMEs and particle acceleration sites in the inner heliosphere.

The arms themselves consist of a polyimide film on which electrically-short dipole antennas are deposited, and they hold the transmission system for sending the electrical signals back to the central electronics package (CEP), located at the intersection of the arms. We have conducted two initial tests of the ROLSS antenna concept. The first test was a comparison of the feed point impedance of a polyimide-film based antenna lying directly on the (terrestrial) ground with results from antenna modeling software, and the second consisted of exposing a polyimide film sample to a simulated lunar environment. The former test showed considerable agreement between the measured and modeled feed-point impedances as a function of frequency, while the latter showed the polyimide film to be robust against the large temperature swings and UV exposure on the lunar surface. While our tests are clearly only the first of a series that need to be performed, the initial results are extremely promising.

The array operates over the wavelength range 30–300 m (1–10 MHz), with a selectable, variable frequency sub-band being able to be placed anywhere within the operational wavelength range. The receivers and associated electronics (e.g., command and data handling electronics, power supply electronics) would be located in a central electronics package (CEP) in order to minimize the power distribution, thermal management, and electromagnetic interference (EMI) shielding issues. The CEP should be able to be carried in a standard lunar lander carrier, but multiple designs are possible, depending upon whether the rolls of polyimide film are to be transported within the CEP as well or in their own separate containers. When deployed, the nominal CEP design stands approximately 1 m above the lunar surface in order to minimize dust contamination.

While radio frequency (RF) receivers for the ROLSS band have been flown before, the ROLSS receivers would probably require additional development. In particular, it would be desirable to sample the entire waveform (perhaps after some initial filtering) and telemeter the full data stream to Earth. However, while the required high-speed analog-to-digital converters (ADC) either exist or soon will exist, this receiver design would likely also require additional analog components. Considerable development of lower power analog electronics capable of withstanding the lunar temperature extremes is needed.

The prime science mission for ROLSS favors an equatorial site, as a polar site would require that one or more arms of ROLSS be (significantly) longer than the nominal 1000 m length in order to compensate for the foreshortening of the array and maintain the same angular resolution. The site itself should be of relatively low relief topography (e.g., the surface of a mare vs. the highlands), but the entire site does not have to be flat as the fraction of the area occupied by the antenna arms is relatively small. The main deployment tasks would consist of unrolling the antenna arms, connecting the antennas arms to the CEP, and

setting up the solar power array. Deployment could be conducted via a robotic rover, a human-crewed rover, or some combination of both.

The key technologies that need to be developed further in order to enable ROLSS are (1) the polyimide film antennas; (2) ultra-low power electronics, both digital and analog, with the capability to withstand large temperature swings; (3) batteries capable of surviving and operating over larger temperature ranges than currently used for spacecraft missions; and (4) rovers, particularly if an entirely robotic mission is to be contemplated.

Finally, our focus has been on the study of the inner heliosphere via the ROLSS array on the near-side. However, the ROLSS array would also be a natural precursor to a future, larger radio telescope on the far side of the Moon for the study of astrophysics and cosmology (Carilli et al., 2007; Lazio et al., 2007, 2009).

Acknowledgements

We thank J. Schmidt for helpful discussions about the implementation of CME models for ROLSS, the crew of the GSFC IDL for their assistance in refining the design, and the editor for her patience and assistance in making sure that this manuscript was published. Part of this research was carried out at the Jet Propulsion Laboratory, California Institute of Technology, under a contract with the National Aeronautics and Space Administration. The ROLSS concept study was funded by the NASA Lunar Sortie Science Opportunities (LSSO) program. The LUNAR consortium is funded by the NASA Lunar Science Institute (via Cooperative Agreement NNA09DB30A) to investigate concepts for astrophysical observatories on the Moon.

References

- Bale, S.D., Reiner, M.J., Bougeret, J.-L., et al. The source region of an interplanetary type II radio burst. *Geophys. Res. Lett.* 26, 1573–1576, 1999.
- Bauer, S.J. Limits to a lunar ionosphere. *Sitzungsberichte und Anzeiger, Abt. 2* 133, 17–21, 1996.
- Biermann, P.L., Ahn, E.-J., Kronberg, P.P., Medina-Tanco, G., Stanev, T. A possible nearby origin for the highest-energy events observed, in: Lemoine, M., Sigl, G. (Eds.), *Physics and Astrophysics of Ultra-High-Energy Cosmic Rays*, Lecture Notes in Physics, vol. 576. Springer, Berlin, pp. 181–195, 2001.
- Bougeret, J.-L., Kaiser, M.L., Kellogg, P.J., et al. Waves: the radio and plasma wave investigation on the wind spacecraft. *Space Sci. Rev.* 71, 231–263, 1995.
- Cairns, I.H. Solar, interplanetary, planetary, and related extra-solar system science for LOFAR. *Planet. Space Sci.* 52, 1423–1434, 2004.
- Cane, H.V., Erickson, W.C., Prestage, N.P. Solar flares, type III radio bursts, coronal mass ejections, and energetic particles. *J. Geophys. Res. (Space Phys.)* 107 (A10), SSH 14-1, 1315–1334, 2002.
- Carilli, C.L., Hewitt, J.N., Loeb, A. Low frequency radio astronomy from the moon: cosmic reionization and more. Available from: <arXiv:astro-ph/0702070>, 2007.
- Carilli, C.L., Perley, R.A., Dreher, J.W., Leahy, J.P. Multifrequency radio observations of Cygnus A—spectral aging in powerful radio galaxies. *Astrophys. J.* 383, 554–573, 1991.
- Cho, K.-S., Lee, J., Moon, Y.-J., Dryer, M., Bong, S.-C., Kim, Y.-H., Park, Y.D. A study of CME and type II shock kinematics based on coronal density measurement. *Astron. Astrophys.* 461, 1121–1125, 2007.
- Dickey, J.O., Bender, P.L., Faller, J.E., et al. Lunar laser ranging: a continuing legacy of the Apollo Program. *Science* 265, 482–490, 1994.
- Ebenezer, E., Ramesh, R., Subramanian, K.R., SundaraRajan, M.S., Sastry, Ch. V. A new digital spectrograph for observations of radio burst emission from the Sun. *Astron. Astrophys.* 367, 1112–1116, 2001.
- Eilek, J.A., Hughes, P.A. Particle acceleration and magnetic field evolution, in: Hughes, P.A. (Ed.), *Beams and Jets in Astrophysics*. Cambridge University Press, Cambridge, UK, pp. 428–483, 1991.
- Erickson, W.C. The Bruny Island radio spectrometer. *Pub. Astron. Soc. Aust.* 14, 278–282, 1997.
- Gopalswamy, N., Yashiro, S., Krucker, S., Stenborg, G., Howard, R.A. Intensity variation of large solar energetic particle events associated with coronal mass ejections. *J. Geophys. Res. (Space Phys.)* 109 (A12), A12105–A12123, 2004.
- Gopalswamy, N., Yashiro, S., Kaiser, M.L., Howard, R.A., Bougeret, J.-L. Interplanetary radio emission due to interaction between two coronal mass ejections. *Geophys. Res. Lett.* 29 (8), 1265–1268, 2002.
- Gopalswamy, N., Yashiro, S., Kaiser, M.L., Howard, R.A., Bougeret, J.-L. Radio signatures of coronal mass ejection interaction: coronal mass ejection cannibalism? *Astrophys. J.* 548, L91–L94, 2001.
- Gopalswamy, N., Kundu, M.R., Szabo, A. Propagation of electrons emitting weak type III bursts in coronal streamers. *Solar Phys.* 108, 333–345, 1987.
- Harris, D.E., Krawczynski, H. X-ray emission from extragalactic jets. *Ann. Rev. Astron. Astrophys.* 44, 463–506, 2006.
- Harris, D.E. From Clark Lake to Chandra: closing in on the low end of the relativistic electron spectra in extragalactic sources, in: Kassim, N.E., Pérez, M.R., Junor, W., Henning, P.A. (Eds.), *From Clark Lake to the Long Wavelength Array: Bill Erickson's Radio Science*. Astron. Soc. Pacific, San Francisco, pp. 254–263, 2005.
- Holman, G.D., Pesses, M.E. Solar type II radio emission and the shock drift acceleration of electrons. *Astrophys. J.* 267, 837–843, 1983.
- Jones, D.L. Low-mass transmission lines for a lunar low frequency array, in: *IEEE Aerospace Conference*, 2011.
- Jones, D.L., Allen, R.J., Basart, J.P., et al. The ALFA medium explorer mission. *Adv. Space Res.* 26, 743–746, 2000.
- Kim, Y.-H., Bong, S.-C., Park, Y.-D., Cho, K.-S., Moon, Y.-J. Near-simultaneous observations of X-ray plasma ejection, coronal mass ejection, and type II radio burst. *Astrophys. J.* 705, 1721–1729, 2009.
- Lara, A., Gopalswamy, N., Nunes, S., Muñoz, G., Yashiro, S. A statistical study of CMEs associated with metric type II bursts. *Geophys. Res. Lett.* 30 (12), SEP 4-1, 8016–8019, 2003.
- Lazio, T.J.W., Cohen, A.S., Kassim, N.E., Perley, R.A., Erickson, W.C., Carilli, C.L., Crane, P.C. Cygnus A: a long-wavelength resolution of the hot spots. *Astrophys. J.* 642, L33–L36, 2006.
- Lazio, J., Macdowall, R.J., Burns, J., Demaio, L., Jones, D.L., Weiler, K.W. Radio Wavelength Observatories within the Exploration Architecture. Available from: <arXiv:astro-ph/0701770>, 2007.
- Lazio, J., Neff, S., Hewitt, J., et al. Technology Development for the Lunar Radio Array. *Astro2010: The Astronomy and Astrophysics Decadal Survey*, Technology Development Papers, No. 50, 2009.
- Leblanc, Y., Dulk, G.A., Bougeret, J.-L. Tracing the electron density from the corona to 1 AU. *Solar Phys.* 183, 165–180, 1998.
- Lesch, H., Birk, G.T. Particle acceleration by magnetic field-aligned electric fields in active galactic nuclei. *Astron. Astrophys.* 324, 461–470, 1997.
- MacDowall, R.J., Desch, M.D., et al. Microsat and lunar-based imaging of solar radio bursts, in: Rucker, H.O., Kurth, W.S., Mann, G. (Eds.), *Planetary Radio Astronomy VI*. Austrian Academy of Sciences Press, Vienna, pp. 491–504, 2006.
- MacDowall, R.J., Bale, S.D., Demaio, L., et al. Solar imaging radio array (SIRA): a multispacecraft mission, in: Komar, G.J., Wang, J., Kimura, T. (Eds.), *Enabling Sensor and Platform Technologies for Spaceborne Remote Sensing: Proceedings of the SPIE*. SPIE, Vol. 5659, p. 284, 2005.

- MacDowall, R.J., Lara, A., Manoharan, P.K., et al. Long-duration hectometric type III radio bursts and their association with solar energetic particle (SEP) events. *Geophys. Res. Lett.* 30 (12), SEP 6-1, 8018-8021, 2003.
- Mann, G., Jansen, F., MacDowall, R.J., Kaiser, M.L., Stone, R.G. A heliospheric density model and type III radio bursts. *Astron. Astrophys.* 348, 614–620, 1999.
- Mann, G., Luehr, H. Electron acceleration at quasi-parallel shocks in the solar corona and its signature in solar type II radio bursts. *Astrophys. J. Suppl.* 90, 577–581, 1994.
- Oberoi, D., Matthews, L.D., Cairns, I.H., et al. First spectroscopic imaging observations of the sun at low radio frequencies with the Murchison widefield array prototype. *Astrophys. J.* 728, L27, 2011.
- Perley, R.A. Wide field imaging II: imaging with non-coplanar arrays, in: Perley, R.A., Schwab, F.R., Bridle, A.H. (Eds.), *Synthesis Imaging in Radio Astronomy*, Astron. Soc. Pacific, San Francisco, pp. 259–275, 1989.
- Ramesh, R., Kathiravan, C., Sundararajan, M.S., Barve, I.V., Sastry, C.V. A low-frequency (30–110 MHz) antenna system for observations of polarized radio emission from the solar corona. *Solar Phys.* 253, 319–327, 2008.
- Reasoner, D.L., O'Brien, B.J. Measurement on the lunar surface of impact-produced plasma clouds. *J. Geophys. Res.* 77, 1292–1299, 1972.
- Richardson, I.G., Lawrence, G.R., Haggerty, D.K., Kucera, T.A., Szabo, A. Are CME 'interactions' really important for accelerating major solar energetic particle events? *Geophys. Res. Lett.* 30, 120000–120001, 2003.
- Sawant, H.S., Gergely, T.E., Kundu, M.R. Positions of type II fundamental and harmonic sources in the 30–100 MHz range. *Solar Phys.* 77, 249–254, 1982.
- Schmidt, J.M., Gopalswamy, N. Synthetic radio maps of CME-driven shocks below 4 solar radii heliocentric distance. *J. Geophys. Res.* 113 (A8), CiteID A08104–A08119, 2008.
- Shanmugaraju, A., Moon, Y.-J., Vrsnak, B. Type II radio bursts with high and low starting frequencies. *Solar Phys.* 254, 297–310, 2009.
- Vyshlov, A.S. Preliminary results of circumlunar plasma research by the Luna 22 spacecraft, in: *Space Research XVI, Proceedings of the Open Meetings of Workshop Groups of Physical Sciences*. Akademie-Verlag, p. 945, 1976.
- Vyshlov, A.S., Savich, N.A. Observations of radio source occultations by the moon and the nature of the plasma near the moon. *Cosmic Res.* 16, 450–454, transl. *Kosmicheskie Issledovaniya*, 16, 551–556, 1978.
- Weiler, K.W. *The Low Frequency Space Array*, NASA Proposal (Principal Investigator), 1986
- Weiler, K.W., Johnston, K.J., Simon, R.S., Dennison, B.K., Spencer, J.H., Erickson, W.C., Kaiser, M.L., Cane, H.V., Desch, M.D., Hammarstrom, L.M. A low frequency radio array for space. *A&A* 195, 372–379, 1988.